



Original Paper

<http://ajol.info/index.php/ijbcs>

<http://indexmedicus.afro.who.int>

Comprehensive analysis of nutritional composition, mineral content, antimicrobial activity, and theoretical evaluation of phytochemicals in henna (*Lawsonia inermis*) from the Fujairah, United Arab Emirates

Amal Salem Khamis Hamad ALSAMAHI, Hajer Ali Abdulla ALHMOUDI,
Shaher Bano MIRZA* and Fouad Lamghari RIDOUANE

Fujairah Research Centre, Sakamkam Road, Fujairah, United Arab Emirates.

**Corresponding author; E-mail: shaher.bano@frc.ae ; Phone: +971 508011873*

Received: 07-09-2023

Accepted: 17-11-2023

Published: 31-12-2023

ABSTRACT

Henna (*Lawsonia inermis*) is a versatile that has been highly regarded for centuries due to its cultural and medicinal significance. Henna boasts a rich array of phytochemicals, each contributing to its numerous therapeutic benefits. This study provided a comprehensive assessment of the henna plant and aimed to explore the potential of phytochemicals as candidates for drug development through various analyses including nutritional and mineral composition, antimicrobial activity, docking analysis, and theoretical ADMET (Absorption, Distribution, Metabolism, Excretion and Toxicity), toxicity, and druglikeness evaluation. The 2 plants Samples collected from 2 different locations in Fujairah emirate exhibited significant amount of Potassium, Magnesium, and calcium, making them a valuable source of essential minerals. The nutritional and mineral content of the sample was measured using international standard methods (Association of Official Analytical Chemists; AOAC 2001.11, AOAC 920.39, AOAC 962.29, and AOAC 942.05). Antimicrobial assessment done by disc diffusion method revealed potent antibacterial activity against *Bacillus cereus* and *Staphylococcus aureus* with inhibition of 30-32 mm and 15-20 mm, respectively, Similarly, it shows antifungal activity against *Aspergillus flavus* and *Candida albicans* with inhibition of 9-10 mm and 11-12 mm, respectively. Docking analysis provided insights into the interactions between henna phytochemicals and AcuA protein which elucidate the higher interactions of Agrimonolide-6-O-glucopyranoside with binding pocket and surrounding residues with highest binding energy. Similarly, the theoretical ADMET, toxicity, and drug likeness analysis highlighted Agrimonolide-6-O-glucopyranoside as a promising compound for drug development as well. These findings hold promise for henna plant and Agrimonolide-6-O-glucopyranoside's potential use as a natural alternative to conventional antimicrobial agents. However, additional studies are needed to assess the safety, efficacy, and potential mechanisms of action of these phytochemicals in the henna plant extract.

© 2023 International Formulae Group. All rights reserved.

Keywords: *Lawsonia inermis*, Henna, nutritional composition, antimicrobial activity, docking, ADMET analysis, druglikeness

INTRODUCTION

Henna (*Lawsonia inermis*) is a versatile plant that is well-known for its cultural significance, medicinal properties, and

extensive range of applications. Belonging to Lythraceae plant family it is a plant with spine-tipped branches that can reach heights between 2 and 6 meters. The semi-sessile leaves have an

elliptical shape and a broad lance-like form. As depicted in Figure 1, the dorsal side of the foliage contains visible lines. The plant's adaptability to the harsh soil conditions, including extreme alkalinity and acidity, is extraordinary. The optimal temperature range for henna growth is between 19°C and 27°C, however, it can thrive in harsh climate as well. Originating in arid regions, henna is profoundly rooted in the traditions and heritage of numerous cultures, including the United Arab Emirates (UAE). Numerous plants have been assessed for their therapeutic potential in treating various ailments around the world for centuries, encompassing both historical practices and contemporary cultures. The evaluation extends not only to their medicinal properties but also to their diverse applications and uses (Nana et al., 2023; Fodouop et al., 2020; Ballo et al., 2020). Henna has been valued for centuries for its medicinal properties, as it contains a variety of phytochemicals that contribute to its therapeutic effects (Pasandi Poor et al., 2018).

Henna leaves possess significant antimicrobial and antifungal properties, making them a valuable natural resource for combating microbial infections. The antimicrobial importance of henna leaves has been attributed to the presence of various bioactive compounds, including fraxetin, dihydrodehydrodiconiferyl alcohol, lawsoniaside, 2-methoxy-3-methyl-1-butene, agrimonolide-6-O-glucopyranoside, coumarin, and gallic acid. These compounds contribute to the plant's medicinal properties, including anti-

inflammatory, antimicrobial, antioxidant, hepatoprotective, anticancer, and anti-inflammatory effects (Babu and Subhasree, 2009). The presence of bioactive compounds in henna leaves contributes to its antimicrobial effectiveness, making it a valuable resource for natural and alternative antimicrobial strategies. Additional study and investigation of henna's antimicrobial potential can pave the way for the development of novel antimicrobial agents to combat microbial infections and address the challenges of antibiotic resistance. The exploration of these phytochemicals can further enhance our understanding of the therapeutic potential of henna and supports its traditional use in various cultures (Semwal et al., 2014; Arya et al., 2006; Sakkir et al., 2012).

With a thorough understanding of the significance of the henna plant, the purpose of this study was to investigate its nutritional and mineral content, as well as to conduct antimicrobial evaluations. The antimicrobial evaluation will be followed by docking experiments concentrating on the interaction between the phytochemicals present in henna plants and the targeted microbial proteins. Through this comprehensive approach, evaluation of the theoretical potential of these phytochemicals and propose them as potential therapeutic agents for the formulation of antimicrobial products, including topical creams, ointments, and disinfectants, thereby enhancing our understanding of the therapeutic properties of henna and its potential medical applications was intended.



Figure 1: Henna tree and leaves.

MATERIALS AND METHODS

Plant materials

Fresh *Lawsonia inermis* leaves were collected from two different regions in Fujairah, Dedna and Dibba. The sample weigh about 500 g and kept it in sterile Plastic Packaging.

Chemical analysis

The dry Matter, crude protein, crude Fat, crude fiber, ash, TDN (Total digestible nutrients) and tannin content were determined by international standard procedures (Association of Official Analytical Chemists, AOAC 2001.11, AOAC 920.39, AOAC 962.29, AOAC 942.05).

Mineral analysis

The major minerals, comprising calcium, phosphorus, sodium, potassium, zinc, Copper, manganese, selenium and magnesium were determined according to the Gravimetry, HPLC (High-performance liquid chromatography), Soxhlet extraction and ICP-OES (Inductively Coupled Plasma Optical Emission spectroscopy) (AOAC 962.09, AOAC 941.12) methods.

Sample preparation for nutrient, chemical composition

According to international standard procedures, the chemical components of dry matter, crude protein, crude fat, crude fiber, ash, TDN, total sugars, and mineral analyses were identified as mentioned in Al Dahmani et al. (2023) and Al Dhanhani et al. (2023). In this investigation, high-quality, analytical-grade chemicals were used to detect nutrients, minerals, and heavy metals. The dirt was removed from the leaf samples by washing them in sterile water. The 0.1-gram samples were measured and then finely powdered. After that, 5 ml of 69% HNO₃ (nitric acid) was used to wash the samples for 10 minutes at 200°C in a Teflon vessel. The leaves were then digested by mixing 7 ml of 69% HNO₃ with 1 ml of 31% H₂O₂. The entire operation was carried out using a rotor. After washing with deionized water, the teflon vessel was carefully removed

from the rotor. The digested leaves were rinsed three to four times with deionized solution on filter paper, and the resulting master sample solution was used to conduct the analysis. In the meantime, a blank solution devoid of any reagents was also made. As stated in C. Naumann and R. Bassler, "Chemical Analyses of Animal Feed," VDLUFA-Verlag, Darmstadt, 2004, dry matter was determined using gravimetry, crude fat by Soxhlet, crude protein by Kjeldahl method, sugar by HPLC, crude fiber and TDN by standard method AOAC 941.12, and ash by AOAC 962.09. Standard techniques in the ICP-OES technology have been used to analyze minerals for calcium, phosphorus, sodium, potassium, zinc, copper, manganese, selenium, magnesium, and heavy metals. Handling samples ensures homogeneity (Akhtar et al., 2021).

Info graphical representation and comparison of the laboratory analysis between all three sites has been accomplished using Microsoft excel.

Microbiological analysis

The antibacterial and antifungal assays were determined by Disk Diffusion Method (ISO 16782:2016). *Staphylococcus aureus* 6538, *Bacillus cereus* 6633, *Methicillin-Resistant Staphylococcus aureus* MP-2, *Pseudomonas aeruginosa* 10145, *Escherichia coli* 8739 were the bacterial strains used and *Aspergillus flavus* 16883, and *Candida albicans* 10231 were the fungal strains. All microbes were purchased from American Type Culture Collection (ATCC). On Mueller Hinton agar, the antibacterial activity of crude *L. inermis* extracts was evaluated using the agar disc diffusion method (Ibrahim et al., 2021a). Bacterial inoculum was made by suspending colonies from a 24-hour culture in 9 ml of sterile distilled water saline. A spectrophotometer (DO= 0.08 to 0.1 at 625nm) was used to modify the cell density of each inoculum to achieve a final concentration of around 10⁸ CFU/ml (0.5 McFarland standard). In this approach, a 10⁸ CFU/ml inoculum was dispersed over the surface of a 3-4 mm thick

Mueller-Hinton agar. Whatman paper discs N° 3 of 6 mm diameter containing 10 µl of crude *L. inermis* extracts dissolved in 100% DMSO were put to the plate after drying (no more than 15 minutes). After 24 hours of incubation at 37°C, the inhibitory zone diameter in mm was measured to determine activity. The antifungal activity was tested in the same manner as bacteria, with the exception that the culture medium used was Mueller Hinton + 2% glucose + 0.5 g/ml methylene blue/ pH 7.4. A spectrophotometer was used to regulate the cell density of the inoculum (DO = 0.12 to 0.15 at 530 nm). The reading was carried out exactly as indicated for the bacterium. As reference antimicrobials, ciprofloxacin, gentamycin, and amphotericine B were utilized. As a negative control, pure solvent was employed. Antimicrobial activity is assessed beginning with a diameter of 6 mm or greater and is classed as follows:

Very Strong activity: diameter \geq 30 mm;
Strong activity: diameter between 21-29 mm;
medium activity: diameter between 16-20 mm;
Weak activity: diameter between 11-15 mm;
Small or no activity: diameter \leq 10 mm (Al-Rubiay et al., 2008).

In-silico analysis

Ligand and Protein structure Preparation

The phytochemicals of *L. inermis* reported in literature were chosen for this study to evaluate their potential to prevent the spread of infectious diseases. The structures of seven reported phytochemicals were selected for further investigation (Florence et al., 2015). These phytochemicals consisted of Fraxetin, Dihydrodehydrodiconiferyl alcohol, Lawsoniaside, 2-Methoxy-3-methyl-1-butene, Agrimonolide-6-O-glucopyranoside, Coumarin, and Gallic Acid. The 3D structures of the chosen phytochemicals were obtained from PubChem in SDF format. They were converted to PDB format using Convert by ChemAxon. Using Autodock Tools 4.2.6, the selected ligands were prepared for docking in PDBQT format by stabilizing charges and adding polar hydrogen (Yusuf, 2016).

For docking simulations, the AlfaFold predicted three-dimensional structure of the Acetoin utilization protein AcuA (UniProt ID: Q72Z67) from *Bacillus cereus* has been downloaded. The protein encoded by the acetoin utilization gene, AcuA, belongs to the acetyltransferase family, its function includes the acetoin degradation, which is part of ketone degradation. This is 214 residue long protein with single domain, Acetyltransf 1. Binding site residues of the AcuA protein include Asp42, Ile44, Ala45, Phe46, Arg47, Gln52, Ala55, Ile59, Thr81, Leu83, Asp86, Glu89, Glu101, Gly103, Ala104, Ile105, Glu106, Val107, Pro109, Phe111, Arg112, Gly113, Cys114, Ala115, Val116, Gly117, Lys118, Thr138, Glu139, Tyr140, Trp142, His143, Trp144, Asp145, Gln148, Thr149, Leu151, Tyr156, Val159, Met160, Met163, Glu17. When developing antibiotics to combat *Bacillus cereus*, this protein is thought to be the ultimate target. Further the downloaded structure was prepared for docking by removing water molecules and adding polar - Hydrogen, in Autodock Tools 4.2.6. Moreover, 2.0 Kuhlman charges were added and the structure was converted to PDBQT format.

Docking Simulation

Phytoligands, which are “flexible”, were docked into protein targets, which are “rigid”, using AutoDock vina 1.1.2. AutoDock Vina is a powerful and user-friendly docking software that quickly processes data, estimates binding sites, and automatically calculates the size of grid boxes.

For each ligand, a .txt file containing grid box configuration features was generated and saved. A series of codes (commands) were typed into the command prompt to initiate the docking analysis and provide the output score. Binding energy was expressed as a number of kilocalories per mole of protein in the study's results, and the ligand with the maximum negative value was deemed to have the strongest affinity for its target protein. The best fitting model selection was done based on various criteria. Highest number bonds with relatively high binding energy were taken into consideration to select a protein ligand

complex. Autodock Tools visualization was used to display the interaction profiles in 2D for evaluation (Sen et al., 2023).

Theoretical Pharmacokinetics and toxicological profiling

Pharmacokinetic profiling of the ligands was achieved using PreADMET 2.0 which is a web-based application for predicting ADME data using in-silico approach. Various functions are utilised including ADMET, Toxicity, and Druglikeness analysis. For this purpose, 2D structures of the phytochemicals were uploaded to the tool which virtually calculates 19 ADME properties, 12 toxicity endpoints, and 11 druglikeness properties.

RESULTS

Nutritional and micromineral analysis

The proximal nutritional composition of Henna plants is presented in Table 1. The analysis revealed that both samples had similar dry matter content, with Sample 1 (Dedna) exhibiting a slightly higher value of 28.76% compared to Sample 2 (Dibba) with 23.11%. In terms of crude protein, Sample 2 showed a slightly higher value of 4.06% compared to Sample 1 with 3.83%. Both samples had negligible levels of crude fat, with values below the detectable limit (<0.1%). Similarly, both the samples show slight difference in the values for crude fiber, ash content and total sugar. The TDN (Total Digestible Nutrients) value, an indicator of the potential energy available to the animal, was higher in Sample 1 with 27.24% compared to Sample 2 with 21.73%. Furthermore, the analysis revealed the presence of tannins in both samples, with Sample 1 showing a higher tannin content of 9.56% compared to Sample 2 with 7.49%. These findings highlight the potential of henna plants as a source of vital nutrients and offer insightful information about the nutritional makeup of henna plants.

The mineral content analysis of both samples of Henna leaves are listed in Table 2. The most prevalent microelement was potassium, which was found in amounts of roughly 325.6 mg/100g in Sample 1 and 495.05 mg/100g in Sample 2. The amount of sodium,

zinc and manganese are also noteworthy. However, Copper was found in Sample 1 in trace amount and was not detected in Sample 2. Also, trace amounts of manganese were detected in both samples. Phosphorus showed values of 46.52 and 76.12 mg/100g in both samples, respectively. The Mg concentration was observed as 74.62 and 56.2 mg/100g in both samples, respectively.

Antimicrobial activity assessment

The microorganisms subjected to the antibacterial testing were shown to be inhibited to varied degrees (Table 3). *Staphylococcus aureus* showed a modest sensitivity to the henna plant extract, with a zone of inhibition of 15 mm in sample 1 as well as 20mm for Sample 2. The zone of inhibition for *Bacillus cereus* was significantly bigger, at 30 mm in sample 1 and 32 mm in sample 2, indicating a higher susceptibility to the antimicrobial chemicals found in henna. The zone of inhibition for *Methicillin-Resistant Staphylococcus aureus* (MRSA) was just 6 mm and 7mm both samples, respectively, in diameter, indicating that MRSA is less sensitive to the henna leaves. Zones of inhibition for *Pseudomonas aeruginosa* and *Escherichia coli* were in the range of 8-10 mm, and 11-12 mm for both samples, respectively, indicating moderate sensitivity.

In the antifungal assay, the henna plant extract exhibited inhibitory activity against the tested fungal strains. The antifungal chemicals in henna were only moderately effective against *Aspergillus flavus*, with a zone of inhibition measuring 9 and 11mm in both samples, respectively. In contrast, the zone of inhibition measured 11 mm for *Candida albicans* for plant sample 1 and 13 mm for Sample 2, demonstrating that this strain was more sensitive to the henna plant extract's antifungal effects.

Docking simulations

The process of drug discovery relies heavily on the identification of drug-protein interactions. Along with its intended function, it can also reveal any unintended drug effects

or therapeutic benefits. The phytochemical's antibacterial activity was further evaluated utilizing an in-silico method for further clarity. Details such as the chemical formula, atomic weight, and 2D structure are listed in Table 4. *Bacillus cereus* (activity: 32 mm), the organism chosen for further in silico investigation, showed the highest antibacterial activity.

Agrimolide-6-O-glucopyranoside and Lawsoniaside showed the most promising binding affinities and interactions with the Acetoin utilization protein AcuA among the investigated phytochemical substances from the *L. inermis*.

The binding energy of agrimolide-6-O-glucopyranoside was measured to be -9.5 kcal/mol, indicating a very strong interaction with the target protein (Table 5; Figure 2 and 3). Hydrogen bonds were established between this chemical and VAL116, a key amino acid residue at the binding site. Additionally, Agrimolide-6-O-glucopyranoside engaged in multiple interactions with THR137, ILE105, PHE46, ASP145, ARG112, PHE111, VAL107, VAL116, CYS114, GLY113, ALA115, and LYS118. These findings suggest the potential of Agrimolide-6-O-glucopyranoside as a promising lead compound for further exploration and development as a therapeutic agent.

Similarly, Lawsoniaside also exhibited a strong binding affinity with a binding energy of -9.1 kcal/mol. It formed hydrogen bonds with GLY117, GLY113, and THR137, indicating a stable interaction with the AcuA protein. Lawsoniaside also displayed interactions with LEU102, HIS143, TYR156, MET163, ILE105, ALA104, MET163, VAL116, ALA115, ARG112, and VAL107. These findings imply that Lawsoniaside has the potential to be a bioactive molecule and call for more research into its pharmacological uses.

Theoretical Pharmacokinetics and toxicological profiling

ADMET Analysis

Agrimolide-6-O-glucopyranoside, among the tested phytochemicals, demonstrated favorable drug development

properties (Table 6). It possesses a high blood-brain barrier permeability (BBB Permeability: 0.0510216), indicating its ability to enter the central nervous system. The compound exhibits moderate buffer solubility (34.244 mg/L) and favorable Caco-2 (Carcinoma of Colon-2) permeability (16.9307), indicating adequate absorption and distribution properties. In addition, it exhibits inhibitory effects on key metabolic enzymes, including CYP 2C19 (Inhibitor), CYP 2C9 (Inhibitor), and CYP 3A4 (Inhibitor), which may contribute to desired pharmacological effects.

In addition, Agrimolide-6-O-glucopyranoside had a high human intestinal absorption (HIA: 67.706441), indicating efficient intestinal absorption. In addition, it exhibited a low MDCK cell permeability (MDCK Cell Permeability: 0.0659285), which suggests limited efflux by P-glycoprotein (Pgp Inhibition: Non) and potential bioavailability. Also, Agrimolide-6-O-glucopyranoside exhibited moderate plasma protein binding (Plasma Protein Binding: 77.599323) and favorable water solubility (Pure Water Solubility: 135.09 mg/L). These characteristics contribute to its potential as a drug candidate.

In addition, Gallic Acid inhibited CYP 2C19 and CYP 3A4, indicating its potential for modulating drug metabolism. The favorable HIA and Caco-2 permeability of Lawsoniaside indicates efficient absorption and potential bioavailability. Dihydrodehydrodiconiferyl alcohol also inhibited CYP 3A4, an enzyme implicated in the metabolism of numerous drugs. These characteristics are important drug development considerations.

Toxicity analysis

The following are the results of the phytochemical's theoretical toxicity analysis (Table 7). Gallic Acid exhibited a low risk of hERG inhibition, positive results in TA100_NA and TA1535_10RLI, and negative results in TA1535_10RLI and TA100_NA. Agrimolide-6-O-glucopyranoside demonstrated moderate risk in hERG inhibition, positive results in the Ames test, while negative results in the Carcino_Mouse and Carcino_Rat assays. 2-Methoxy-3-methyl-

1-butene displayed a medium risk in hERG inhibition, mutagenicity in the Ames_test, and positive outcomes in the Carcino_Mouse, Carcino_Rat, and TA1535_10RLI assays. Lawsoniaside demonstrated ambiguous hERG inhibition, mutagenicity in the Ames test, and negative results in the Carcino_Mouse and Carcino_Rat assays. dihydrodehydrodiconiferyl alcohol exhibited a moderate risk in hERG inhibition, nonmutagenicity in the Ames test, and negative results in the Carcino_Mouse and Carcino_Rat assays. Coumarin exhibited low risk in the hERG inhibition assay, mutagenicity in the Ames_test, and positive outcomes in the Carcino_Mouse, Carcino_Rat, and TA1535_10RLI assays. Fraxetin exhibited low risk in the inhibition of hERG, mutagenicity in the Ames test, and negative results in the Carcino_Mouse and Carcino_Rat assays. In addition, the phytochemicals exhibited differing levels of toxicity in the algae_at, daphnia_at, medaka_at, and minnow_at assays.

Druglikeness analysis

The drug likeness analysis provides insightful information regarding the phytochemicals' potential to satisfy certain criteria for drug-like properties (Table 8).

Gallic Acid and 2-Methoxy-3-methyl-1-butene violated the CMC-like rule, indicating that, based on specific molecular weight and atom count criteria, they may not be suitable for drug development. Agrimonolide-6-O-glucopyranoside,

dihydrodehydrodiconiferyl alcohol and Coumarin all satisfied the CMC-like rule, indicating that they possess advantageous physicochemical properties.

Gallic Acid, Agrimonolide-6-O-glucopyranoside, Lawsoniaside, and Fraxetin violated the Lead-like rule; however, these compounds can be improved with structure optimisation. Furthermore, Dihydrodehydrodiconiferyl alcohol and Coumarin violated the Lead-like rule, indicating that their binding affinity requires further investigation. Moreover, Agrimonolide-6-O-glucopyranoside, Lawsoniaside, and Fraxetin violated the MDDR-like rule, indicating that they may not possess drug-like properties. Gallic Acid, dihydrodehydrodiconiferyl alcohol, and Coumarin possessed mid-structure characteristics, whereas 2-Methoxy-3-methyl-1-butene complied with the MDDR-like norm.

Except for Lawsoniaside, all phytochemicals tested complied with the Rule of Five, indicating favorable molecular weight, hydrogen bond acceptors, and hydrogen bond donors. Lastly, based on the WDI-like rule, Agrimonolide-6-O-glucopyranoside, 2-Methoxy-3-methyl-1-butene, Lawsoniaside, and Fraxetin violated the rule, indicating that they may not possess the desirable properties of a drug. dihydrodehydrodiconiferyl alcohol and Coumarin met the WDI-like rule, indicating that they may have drug-like properties.

Table 1: Lawsonia inermis Proximal (%) nutritional composition.

Nutrients	Sample 1	Sample 2
Dry matter	28.76	23.11
Crude Protein	3.83	4.06
Crude Fat	<0.1	<0.1
Crude Fiber	2.66	3.28
Ash	1.58	1.46
*Total Sugar	2.39	2.37
TDN	27.24	21.73
Tannin	9.56	7.49

*Total sugar unit is (g/100g).

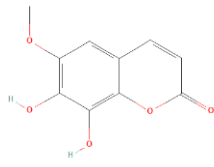
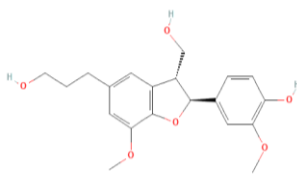
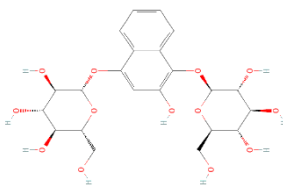
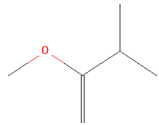
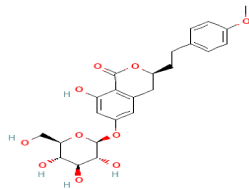
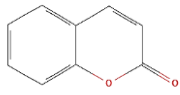
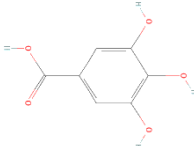
Table 2: Analysis of the minerals in Lawsonia inermis (mg/100g).

Minerals	Sample 1	Sample 2
Calcium	251.04	144.29
Phosphorus	46.52	76.12
Sodium	26.9	29.36
Potassium	325.6	495.05
Zinc	0.42	0.33
Copper	0.13	-
Manganese	1.09	0.67
Selenium	-	-
Magnesium	74.62	56.2

Table 3: Lawsonia inermis (mm) microbiological analysis.

Parameter	Sample 1	Sample 2
Antibacterial Assay		
Staphylococcus aureus	15 mm	20
Bacillus cereus	30 mm	32
Methicillin Resistant Staphylococcus aureus	6 mm	7
Pseudomonas aeruginosa	8 mm	10
Escherichia coli	11 mm	12
Antifungal Assay		
Aspergillus flavus	9 mm	11
Candida albicans	11 mm	13

Table 4: Information related to Phytochemicals belongs to Lawsonia inermis.

Ligands	PubChem CID	Molecular Formula	Molecular Weight	Structure
Fraxetin	CID-5273569	C ₁₀ H ₈ O ₅	208.17g/mol	
dihydrodehydrodiconiferyl alcohol	CID-5280637	C ₂₁ H ₂₀ O ₁₁	448.4g/mol	
Lawsoniaside	CID-189451	C ₂₂ H ₂₈ O ₁₃	500.4g/mol	
2-Methoxy-3-methyl-1-butene	CID-142883	C ₆ H ₁₂ O	100.16g/mol	
Agrimoniolide-6-O-glucopyranoside	CID-130868	C ₂₄ H ₂₈ O ₁₀	476.5g/mol	
Coumarin	CID-323	C ₉ H ₆ O ₂	146.14g/mol	
Gallic_Acid	CID-370	C ₇ H ₆ O ₅	170.12g/mol	

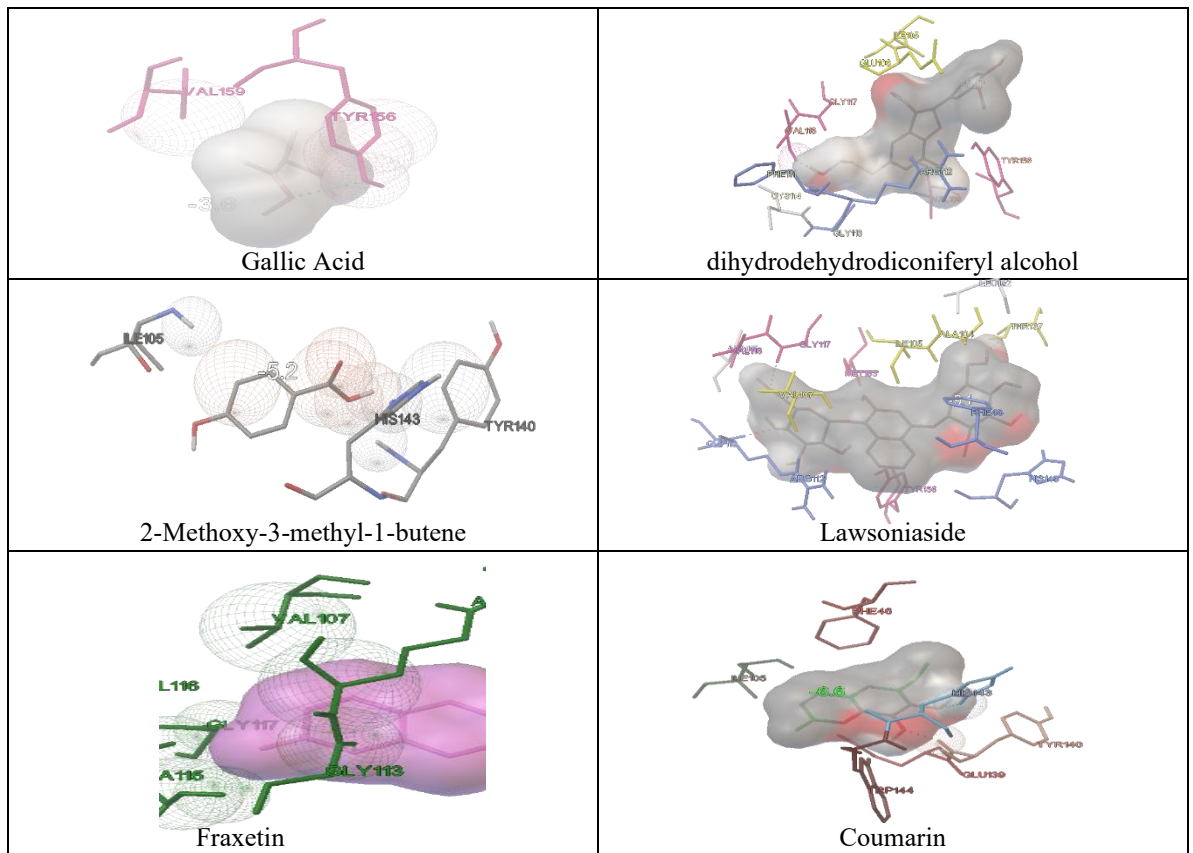


Figure 2: The Phytoligands interactions with the binding pocket residues.

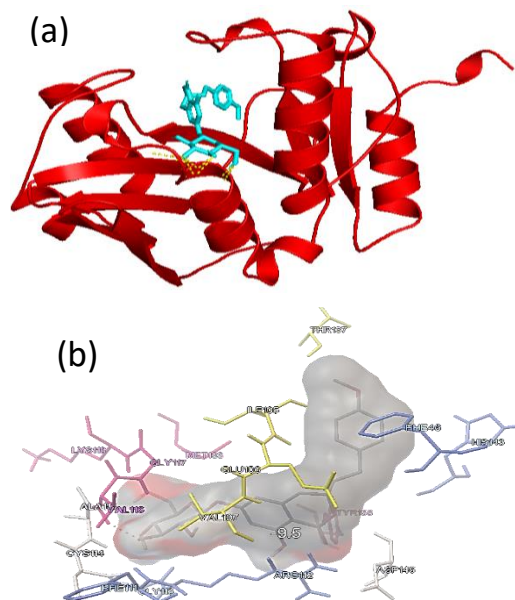


Figure 3: Phytoligand-Protein complex; the Agrimonolide-6-O-glucopyranoside is displayed inside binding pocket of the AcuC protein. (b) the Agrimonolide-6-O-glucopyranoside is making H-bond interaction with VLA116 and other binding pocket residues.

Table 5: Protein-Phytoligand interaction analysis.

No.	Phytochemical name	Docking score	H-bond	Other interactions
1	Gallic Acid	-5.2	TYR140 with HN1 (small green spheres shows H bond)	ILE105, HIS143, TYR140No pi pi no pi cation seen.
2	Agrimolide-6-O-glucopyranoside	-9.5	VAL116	THR137, ILE105, PHE46, ASP145, ARG112, PHE111, VAL107, VAL116, CYS114, GLY113, CYS114, ALA115, LYS118, GLY117
3	2-Methoxy-3-methyl-1-butene	-3.6	TYR156	VAL159
4	Lawsoniaside	-9.1	GLY117, GLY113, THR137	LEU102, HIS143, TYR156, MET163, ILE105, ALA104, MET163, VAL116, ALA115, ARG112, VAL107
5	Dihydrodehydrodiconiferyl alcohol	-8	VAL116	VAL159, TYR156, ILE105, GLY117, ARG112, VAL116, PHE111, CYS114, GLY113
6	Coumarin	-6.6	TYR140, HIS143	GLU139, TRP144, PHE46, ILE105
7	Fraxetin	-5.7	GLY113	VAL107, ARG112, ALA115, GLY117

Table 6: ADMET prediction analysis of Phytoligands using PreADMET Prediction.

ID	Gallic_Acid	Agrimolide-6-O-glucopyranoside	2-Methoxy-3-methyl-1-butene	Lawsoniaside	dihydrodehydrodiconiferyl alcohol	Coumarin	Fraxetin
BBB	0.348084	0.0510216	0.951536	0.0293178	0.248188	0.496494	0.348084
Buffer_solubility_mg_L	1.56124e+006	34.244	744.792	313.203	112.078	117071	1.56124e+006

Caco2	13.8492	16.9307	53.1853	4.50742	22.101	0.212016	13.8492
CYP_2C19_inhibition	Inhibitor	Inhibitor	Non	Inhibitor	Inhibitor	Inhibitor	Inhibitor
CYP_2C9_inhibition	Inhibitor	Inhibitor	Inhibitor	Inhibitor	Inhibitor	Inhibitor	Inhibitor
CYP_2D6_inhibition	Non	Non	Non	Non	Non	Non	Non
CYP_2D6_substrate	Non	Non	Non	Non	Non	Non	Non
CYP_3A4_inhibition	Inhibitor	Inhibitor	Inhibitor	Inhibitor	Inhibitor	Inhibitor	Inhibitor
CYP_3A4_substrate	Non	Weakly	Weakly	Weakly	Substrate	Non	Non
HIA	53.696852	67.706441	100	7.776539	90.049197	86.845015	53.696852
MDCK	9.53976	0.0659285	60.41	0.329053	120.327	121.917	9.53976
Pgp_inhibition	Non	Non	Non	Non	Non	Non	Non
Plasma_Protein_Binding	65.384676	77.599323	88.067899	28.207221	85.138529	38.505826	65.384676
Pure_water_solubility_mg_L	72333.4	135.09	3003.28	1075.61	252.489	9194.3	72333.4
Skin_Permeability	-3.62686	-4.27932	-1.97777	-4.74521	-3.51071	-4.18763	-3.62686
SKlogD_value	0.132480	1.37951	1.77009	-1.62547	2.50741	1.71368	0.132480
SKlogP_value	1.38048	1.37951	1.77009	-1.62547	2.50741	1.71368	1.38048
SKlogS_buffer	0.962710	-4.14346	-2.12866	-3.20354	-3.50727	-0.24997	0.962710
SKlogS_pure	-0.37142	-3.54742	-1.5231	-2.66771	-3.15455	-1.3549	-0.37142

Table 7: Toxicity analysis of Phytoligands using PreADMET Prediction.

ID	Gallic_Acid	Agrimoniolide-6-O-glucopyranoside	2-Methoxy-3-methyl-1-butene	Lawsoniaside	Luteolin-7-O-glucoside	Coumarin	Fraxetin
algae_at	0.0780307	0.0106264	0.0725582	0.0375496	0.0247009	0.0825307	0.0780307
Ames_test	mutagen	mutagen	mutagen	mutagen	non-mutagen	mutagen	mutagen
Carcino_Mouse	negative	negative	positive	negative	negative	negative	negative
Carcino_Rat	positive	negative	positive	negative	negative	positive	positive
daphnia_at	0.689639	0.17244	0.591975	2.89418	0.119766	0.420715	0.689639
hERG_inhibition	low_risk	medium_risk	medium_risk	ambiguous	medium_risk	low_risk	low_risk
medaka_at	0.591427	0.0570044	0.351783	14.319	0.0245045	0.232986	0.591427
minnow_at	0.22656	0.0938967	0.189722	28.4427	0.0436258	0.135639	0.22656
TA100_10RLI	negative	negative	negative	negative	negative	positive	negative
TA100_NA	positive	positive	positive	negative	negative	positive	positive
TA1535_10RLI	positive	negative	positive	negative	negative	positive	positive
TA1535_NA	negative	negative	positive	negative	negative	positive	negative

Table 8: Druglikeness analysis of Phytoligands using PreADMET Prediction.

ID	Gallic_Acid	Agrimolide-6-O-glucopyranoside	2-Methoxy-3-methyl-1-butene	Lawsoniaside	dihydrodehydrodiconiferyl alcohol,	Coumarin	Fraxetin
CMC_like_Rule	Not qualified	Qualified	Not qualified	Not qualified	Qualified	Qualified	Not qualified
CMC_like_Rule_Violation_Fields	AMolRef, No_Total_atoms		Molecular_weight, AMolRef, No_Total_atoms	AlopP98_value, Molecular_weight			AMolRef, No_Total_atoms
CMC_like_Rule_Violations	2	0	3	2	0	0	2
Lead-like_Rule_Violation_Fields	AlopP98_value	Molecular_weight		Molecular_weight, AlopP98_value	Molecular_weight		AlopP98_value
Lead_like_Rule	Violated	Violated	Suitable if its binding affinity is greater than 0.1 microM	Violated	Violated	Suitable if its binding affinity is greater than 0.1 microM	Violated
Lead_like_Rule_Violations	1	1	0	2	1	0	1
MDDR_like_Rule	Mid-structure	Drug-like	Nondrug-like	Drug-like	Drug-like	Mid-structure	Mid-structure
MDDR_like_Rule_Violation_Fields	No_Rings, No_Rotatable_bonds		No_Rings, No_Rigid_bonds, No_Rotatable_bonds			No_Rings, No_Rotatable_bonds	No_Rings, No_Rotatable_bonds
MDDR_like_Rule_Violations	2	0	3	0	0	2	2
Rule_of_Five	Suitable	Suitable	Suitable	Violated	Suitable	Suitable	Suitable
Rule_of_Five_Violation_Fields				Molecular_weight, No_H_bond_acceptors, No_H_bond_donors			
Rule_of_Five_Violations	0	0	0	3	0	0	0

DISCUSSION

The analysis of the nutritional and mineral contents of the henna plant indicates the presence of significant constituents, such as higher level of fiber, total digestible nutrients (TDN), potassium, and calcium. The analysis of two samples collected from distinct locations reveals a subtle difference. The assessment of the antimicrobial activity of the henna plant reveals its broad sensitivity towards both bacterial and fungal assays. The range of activity is slightly different in plant samples collected from different locations from the Fujairah emirate. The slight variation in the activity and nutritional or mineral values for both plant samples can be explained by soil type or water availability to the plants (Agoh et al., 2023). The presence of bioactive compounds with potential antimicrobial properties in the henna plant extract is indicated by the observed inhibitory effects (Ibrahim et al., 2021b). Additional examination may provide a clearer understanding of the specific phytochemicals that are accountable for this observed activity. In order to elucidate the potential molecular candidates responsible for antimicrobial activity, a protein-ligand docking study was conducted on seven phytochemicals, specifically targeting the protein ligands of *Bacillus cereus*.

Lawsoniaside and Agrimonolide-6-O-glucopyranoside have the potential to be important lead compounds in the discovery and development of new drugs due to their significant binding affinities and interactions. The potential therapeutic value of Agrimonolide-6-O-glucopyranoside and Lawsoniaside is indicated by their strong binding affinities and interactions. However, it is important to note that these compounds exhibit multiple interactions with various amino acid residues within the protein's binding site. This suggests a wide range of molecular interactions that may extend beyond the originally intended target. The promiscuous nature of binding interactions can give rise to off-target effects and unintended interactions

with various proteins or biomolecules within the biological system. Consequently, this may lead to the manifestation of adverse reactions or toxicity (Ahamed et al., 2021). Hence, it is crucial to conduct a comprehensive examination of the selectivity and specificity of these compounds before any further drug development. As a result, extensive pharmacokinetic and toxicological profiling has been conducted on these specific phytochemicals.

The analysis of Absorption, Distribution, Metabolism, Excretion, and Toxicity (ADMET) reveals that Agrimonolide-6-O-glucopyranoside exhibits the most favourable overall ADMET profile compared to the other phytochemicals that were tested. In the ADMET study, other phytochemicals also exhibit some favorable characteristics, but Agrimonolide-6-O-glucopyranoside consistently exhibits a more complete set of properties that are favorable for drug development.

In the context of the Toxicity Analysis, it has been observed that Agrimonolide-6-O-glucopyranoside shows a notably low level of toxicity across various assays that have been conducted. The results of the algae and daphnia toxicity tests demonstrate a low level of toxicity, suggesting that the substance under investigation exhibits minimal detrimental impacts on aquatic organisms. Furthermore, it is non-mutagenic in the Ames test and negative in both the Carcino_Mouse and Carcino_Rat tests, suggesting a lower potential for causing cancerous growth. In the Drug Likeness Analysis, it has been determined that Agrimonolide-6-O-glucopyranoside satisfies multiple drug likeness parameters. Despite its violation of the Lead-like Rule, this compound may still be deemed acceptable if its binding affinity exceeds 0.1 microM. However, in our docking experiment, the binding affinity comes as $-1.199 \times 10^{19} \mu\text{M}$. It is important to consider that structural optimization can help the compounds to enhance their selectivity and reduce the risk of side effects. By carefully

designing and synthesizing analogs or derivatives, it may be possible to achieve the desired therapeutic activity while minimizing off-target interactions.

Conclusion

The comprehensive knowledge surrounding the henna plant significantly enhances our understanding of its therapeutic capabilities, thereby facilitating future investigations and advancements in the field of pharmaceutical and cosmetic product development. This accumulated knowledge serves as a foundation for exploring the potential of henna's bioactive compounds in the creation of innovative products. The analysis conducted puts light on the potential of Agrimonolide-6-O-glucopyranoside as a potential therapeutic agent. Further investigations are required to evaluate the safety, efficacy, and potential mechanisms of Agrimonolide-6-O-glucopyranoside.

AUTHOR CONTRIBUTIONS

The authors confirm contribution to the paper as follows: study conception and design: S.B.M and F.L.R; data collection analysis and interpretation of results: A.S.K.H.A, H.A.A.A and S.B.M; draft manuscript preparation: A.S.K.H.A, H.A.A.A and S.B.M. All authors reviewed the results and approved the final version of the manuscript. All authors have read and agreed to the published version of the manuscript.

COMPETING INTERESTS

The authors declare that they have no competing interest.

REFERENCES

Agoh CF, Saley MB, Lekadou TT, Yao SDM, Coffi PMJ, Goula BTA. 2023. Impacts of climate variability on the production of Dwarf x Tall and Tall x Tall coconut (*Cocos nucifera* L.) palm hybrids planted on the coast in Côte d'Ivoire. *International Journal of Biological and Chemical Sciences*, **17**(2): 451-474. DOI: 10.4314/ijbcs.v17i2.14

Ahamed NA, Panneerselvam A, Arif IA, Abuthakir MHS, Jeyam M, Ambikapathy V, Mostafa AA. 2021. Identification of potential drug targets in human pathogen *Bacillus cereus* and insight for finding an inhibitor through subtractive proteome and molecular docking studies. *Journal of Infection and Public Health*, **14**(1): 160–168. DOI: 10.1016/j.jiph.2020.12.005

Akhtar J, Bashir F, Bi S. 2021. Scientific Basis for the Innovative Uses of Henna (*Lawsonia inermis* L) mentioned by Unani Scholars in different ailments. *Int. J Complement Altern Med Res.*, **14**(1): 1–21. DOI: 10.9734/JOCAMR/2021/v14i130234

Al Dahmani WSO, Mirza SB, Kalathingal MSH, Ridouane FL. 2023. Macro-mineral concentration analysis of *Acacia ehrenbergiana* (Salam) from the origin of Fujairah, UAE, with staple food items as a mineral rich dietary supplement for arid and semi-arid lands of the world. *Advancements in Life Sciences*, **9**(4): 534–538.

Al Dhanhani ASSJ, Mirza SB, Ridouane FL, Alhefeiti FRMO. 2023. Investigating the nutritional potential of *Acacia tortilis* and *Acacia ehrenbergiana* from the origin of Fujairah, UAE, for Arabian Tahr as native fodder plants. *Advancements in Life Sciences*, **10**(1).

Al-Rubiay KK, Jaber NN, Al-Mhaawe BH, Alrubaiy LK. 2008. Antimicrobial efficacy of henna extracts. *Oman Medical Journal*, **23**(4): 253. DOI: 10.4236/ojmm.2016.61001

Babu PD, Subhasree RS. 2009. Antimicrobial activities of *Lawsonia inermis*-a review. *Acad J Plant Sci*, **2**(4): 231–232. DOI: 10.4236/oalib.1106371

Ballo M, Somboro AM, Maiga M, Diarra B, Sanogo M, Denou A, Togola, A, Youl EN, Bah S, Sanogo R, Diallo D. 2020. Evaluation of antimycobacterial activity of medicinal plants used by Malian traditional medicine practitioners to treat tuberculosis. *International Journal of Biological and Chemical Sciences*, **14**(9): 3145-3155. DOI: 10.4314/ijbcs.v14i9.14

Florence AR, Sukumaran S, Joselin J, Brintha TS, Jeeva S. 2015. Phytochemical screening of selected medicinal plants of the family Lythraceae. *Biosci Discov.*, **6**(2): 73–82. DOI: 10.1038/s41598-021-89437-4

- Fodouop CSP, Mefokou DY, Tangué BT, Sokoudjou JB, Menoudji ST, Kamsu GT, Gatsing D. 2020. Contribution to the ethnobotanical inventory of medicinal plants used for the treatment of typhoid fever in Adamaoua region, Cameroon. *International Journal of Biological and Chemical Sciences*, **14**(9): 3078-3096. DOI: 10.4314/ijbcs.v14i9.9
- Ibrahim SMS, Rasool CS, Al-Asady AA. 2021. Antimicrobial activity of crude henna extract against Gram-positive bacteria. *MicroMedicine*, **9**(1): 18–26. DOI: 10.5281/zenodo.4569112
- Nana WG, Makemteu J, Petnga JM, Noumi E, Ngome FA, Ambang Z. 2023. Therapeutic recipes based on medicinal plants used for the treatment of Flu, Cold, Cough and Covid-19 at cities of Mbanga and Yaounde (Cameroon). *International Journal of Biological and Chemical Sciences*, **17**(3): 950-961. DOI: 10.4314/ijbcs.v17i3.15
- Pasandi Poor A, Farahbakhsh H, Moradi R. 2018. Assessing effect of climatic-management factors on yield and growth characteristics of henna (*Lawsonia inermis* L.) as a medicinal-industrial plant in Kerman province. *Journal of Agroecology*, **10**(1): 203–217. DOI: 10.22067/JAG.V10I1.56222
- Sakkir S, Kabshawi M, Mehairbi M. 2012. Medicinal plants diversity and their conservation status in the United Arab Emirates (UAE). *J Med Plants Res.*, **6**(7): 1304–1322. DOI: 10.5897/JMPR11.1412
- Semwal RB, Semwal DK, Combrinck S, Cartwright-Jones C, Viljoen A. 2014. *Lawsonia inermis* L.(henna): Ethnobotanical, phytochemical and pharmacological aspects. *Journal of Ethnopharmacology*, **155**(1): 80–103. DOI: 10.1016/j.jep.2014.05.042
- Sen S, Borthakur MS, Chetia D. 2023. *Lawsonia inermis* Linn: A breakthrough in cosmeceuticals. *Sciences of Phytochemistry*, **2**(1): 128–158. DOI: 10.58920/sciphy02010128
- Yusuf M. 2016. Phytochemical analysis and antibacterial studies of *Lawsonia inermis* leaves extract. *J Chem Pharm Res.*, **8**: 571–575. DOI: 10.5829/idosi.ijmr.2013.4.1.6679